Society of Medical Education & Research

2021, Volume 1, Page No: 85-102
ISSN: 3108-4834

Archive of International Journal of Cancer and Allied Science

A Functional Interaction Between rs10204525 and miR-4717-3p Regulates PD-1 Levels and Serves as a Biomarker for Immune-Related Toxicity During Anti-PD-1/PD-L1 Treatment in Advanced Cancer

Emily Rose Carter[1]*, Jonathan Michael Lee[1]

[1]Department of Oncology, School of Medicine, University of Toronto, Toronto, Canada.

***E-mail** ✉ emily.carter.onco@gmail.com

Abstract

Despite widespread clinical use of antibodies targeting programmed cell death-1 (PD-1) and programmed cell death ligand 1 (PD-L1), dependable biomarkers for anticipating immune-related adverse events (irAEs) remain largely unavailable. This investigation examined whether inherited variation within the PD-1 gene could identify patients at increased risk of irAEs following immune checkpoint blockade and clarified the molecular mechanism through which the most relevant variant exerts its biological effects. Clinical data, toxicity profiles, survival outcomes, and peripheral blood samples were obtained from two independent populations: one comprising patients with advanced malignancies receiving anti–PD-1/PD-L1 monotherapy, and a second including patients with advanced non-small cell lung cancer (NSCLC) treated with anti–PD-1 combined with platinum-based chemotherapy, with or without anti–cytotoxic T-lymphocyte antigen 4 (CTLA-4). Six PD-1 single nucleotide polymorphisms (rs2227981, rs7421861, rs11568821, rs36084323, rs2227982, and rs10204525) were genotyped and analyzed for associations with clinicopathological features and irAE incidence. Bioinformatic screening was used to identify microRNAs predicted to interact with the candidate SNP. Allele-dependent miRNA binding and its regulatory impact on PD-1 expression were experimentally assessed in patient-derived peripheral blood mononuclear cells (PBMCs). Functional immune reactivity was examined using co-culture systems in which HLA-matched PBMCs from genotyped patients were incubated with non-malignant human epidermal keratinocytes (HaCaT) or bronchial epithelial cells (BEAS-2B) in the presence of immune checkpoint inhibitors.

No significant association with irAE development was observed for most PD-1 polymorphisms evaluated. In contrast, rs10204525 showed a consistent and statistically significant correlation with both low-grade (1–2) and high-grade (3–4) irAEs in both cohorts. Patients homozygous for the C allele experienced irAEs more frequently than heterozygous carriers. This polymorphism was located within the 3′ untranslated region (3′-UTR) of PD-1 and demonstrated allele-specific interaction with miR-4717-3p. Manipulation of miR-4717-3p levels and disruption of its binding to rs10204525 produced genotype-dependent differences in PD-1 expression and inducibility in PBMCs. These molecular alterations translated into functional consequences, as PBMCs carrying the C/T genotype exhibited diminished capacity to recognize and eliminate HLA-matched non-cancer cells compared with C/C PBMCs, an effect that was accentuated following anti–PD-1 exposure. Independent validation experiments using additional patient-derived PBMCs and combined anti–PD-1/anti–CTLA-4 treatment confirmed these findings across both HaCaT and BEAS-2B co-culture models. This study identifies an rs10204525–miR-4717-3p regulatory axis that governs PD-1 expression and shapes immune cell responsiveness toward non-malignant tissues, establishing rs10204525 as a clinically relevant biomarker for predicting irAEs in patients undergoing anti–PD-1/PD-L1-based immunotherapy.

Keywords: rs10204525, miR-4717-3p, PD-1 Level, Anti-PD-1/PD-L1 treatment, Cancer

Access this article online https://smerpub.com/

Received: 07 November 2020; **Accepted:** 19 February 2021

How to cite this article: Carter ER, Lee JM. A Functional Interaction Between rs10204525 and miR-4717-3p Regulates PD-1 Levels and Serves as a Biomarker for Immune-Related Toxicity During Anti-PD-1/PD-L1 Treatment in Advanced Cancer. Arch Int J Cancer Allied Sci. 2021;1:85-102. https://doi.org/10.51847/aYEtM32NYo

Introduction

The introduction of immune checkpoint inhibitors (ICIs) targeting cytotoxic T-lymphocyte antigen 4 (CTLA-4), programmed cell death-1 (PD-1), and programmed cell death ligand 1 (PD-L1) has substantially reshaped therapeutic strategies for advanced solid malignancies,

including melanoma, head and neck squamous cell carcinoma, non-small cell lung cancer, and renal cell carcinoma [1–14]. Nevertheless, only a fraction of treated patients achieve durable benefit, and clinical success is frequently counterbalanced by immune-related adverse events that may be severe or life-threatening. Consequently, the identification of biomarkers capable of predicting both treatment toxicity and patient susceptibility remains a critical challenge.

Reported rates of severe irAEs range from approximately 10% to 60%, depending on cancer type and immunotherapy regimen [1–11]. These events often mimic autoimmune disorders, can emerge at variable time points, and may involve virtually any organ system [15, 16]. In many cases, irAEs necessitate permanent discontinuation of immunotherapy [1–11, 15, 16]. Although multiple biomarkers have been explored to predict therapeutic efficacy, none have proven reliable for forecasting irAE development [17–24].

Inherited genetic variation plays a pivotal role in determining disease risk, immune regulation, and treatment-related toxicity. Tens of thousands of SNPs have been linked to cancer susceptibility, prognosis, therapeutic response, and adverse drug reactions. Notably, polymorphisms within the PD-1 gene have been associated with autoimmune diseases, including Crohn's disease, systemic lupus erythematosus, type I diabetes, rheumatoid arthritis, and multiple sclerosis [25], as well as with cancer risk [26–31] and antiviral immune control [32]. However, data connecting PD-1 genetic variants to immune checkpoint inhibitor–induced irAEs have been inconsistent. The present study was therefore designed to validate PD-1 SNPs as predictors of irAE risk in patients with advanced cancer treated with PD-1/PD-L1 blockade and to define the molecular mechanisms underlying the effects of the most relevant variant.

Materials and Methods

Study population

This study was conducted without altering routine clinical care and included two separate patient groups. The first group comprised Caucasian individuals with confirmed advanced cancers who received single-agent anti-PD-1/PD-L1 therapy as either first-line or later treatment, recruited between July 2017 and June 2022 at "San Giovanni di Dio e Ruggi D'Aragona" University Hospital. The second group consisted of Caucasian patients with advanced NSCLC who were treated upfront with platinum-based chemotherapy (PBCT) combined with either pembrolizumab (anti-PD-1) or a triple regimen of PBCT, nivolumab (anti-PD-1), and ipilimumab (anti-CTLA-4); recruitment occurred from April 2021 to May 2024 at the same institution.

Patients were eligible if they met the following criteria: age above 18 years, no prior exposure to anti-PD-1/PD-L1 monoclonal antibodies, prednisone-equivalent dose ≤10 mg/day, absence of symptomatic brain metastases, no active autoimmune disease, and provision of informed consent for both clinical-pathological data collection and blood sampling. The first cohort included patients with HNSCC, melanoma, NSCLC, and RCC depending on availability. Both cohorts excluded NSCLC patients harboring tumor alterations in EGFR, ALK, ROS1, BRAF, MET, RET, HER2, or NTRK. Evaluation of these molecular alterations was performed on tumor tissue or via liquid biopsy, following national pathology guidelines.

Clinical data collected comprised age, sex, ECOG performance status (PS), smoking history, comorbidities, presence of asymptomatic brain metastases, and previous systemic treatments. Treatment outcomes assessed included response rate, median progression-free survival (PFS), median overall survival (OS), and incidence of immune-related adverse events (irAEs). To protect patient privacy, a progressive anonymous identification code was assigned to each participant.

Patients continued ICIs (nivolumab or pembrolizumab for anti-PD-1, atezolizumab for anti-PD-L1, and ipilimumab for anti-CTLA-4) until disease progression, unacceptable toxicity, or as clinically indicated in accordance with European Society for Medical Oncology guidelines. irAEs were defined as adverse events with a definite, probable, or possible relationship to ICIs according to CTCAE V.4.0 [33] and graded accordingly; monitoring continued throughout therapy and for 100 days after discontinuation. Radiographic imaging was performed every eight weeks. Tumor responses were assessed using RECIST V.1.1 [34], with results classified as complete response (CR), partial response (PR), stable disease (SD), or progressive disease (PD). The objective response rate (ORR) was calculated as the proportion of patients achieving CR or PR. PFS was measured from treatment initiation to documented PD or death from any cause, while OS was defined as the interval from therapy start to death or last follow-up. Patients who died due to COVID-19 were excluded. The study received approval from the local ethics committee (prot./SCCE n.85275)

and was conducted in accordance with the Declaration of Helsinki.

PD-1 SNP genotyping

Six PD-1 single nucleotide polymorphisms (rs10204525, rs2227981, rs7421861, rs11568821, rs36084323, rs2227982) previously linked to autoimmunity, cancer susceptibility, and prognosis [26–31] were selected for genotyping. Peripheral blood mononuclear cells (PBMCs) were isolated from patients prior to anti-PD-1/PD-L1 therapy as described previously [35] and stored at −80°C. DNA extraction from PBMCs was performed using the Maxwell 16 Blood DNA Purification Kit (Promega, Madison, WI, USA), and the purity and concentration of each sample were measured using a NanoDrop spectrophotometer (Thermo Scientific, Wilmington, DE, USA). SNP genotyping was conducted with TaqMan assays (C_172862_10 for rs10204525, C_57931286_20 for rs2227981, C_26891639_10 for rs7421861, C_57931290_10 for rs11568821, C_57931321_10 for rs36084323, and C_57931287_10 for rs2227982) as described previously [36].

In silico analysis

Annotation of PD-1 SNPs was performed using NCBI dbSNP (http://www.ncbi.nlm.nih.gov/SNP) and ENSEMBL V.58 (http://www.ensembl.org/). Potential microRNAs (miRNAs) targeting the 3′-UTR of PD-1, including rs10204525, were identified using miRNASNP-v4 (https://gong_lab.hzau.edu.cn/miRNASNP/snpdetail). The minimum free energy (MFE) of miRNA binding, representing hybridization strength, was evaluated through the miRTarBase web server (https://awi.cuhk.edu.cn/~miRTarBase/miRTarBase_2025/php/index.php).

Experimental procedures

Isolation and maintenance of cells

Peripheral blood mononuclear cells (PBMCs) were collected from patients enrolled in the study and isolated using standard protocols. These cells were cultured in RPMI-1640 medium (Euroclone, Milan, Italy) supplemented with 10% fetal bovine serum (FBS) and 1% penicillin-streptomycin, under a humidified atmosphere at 37°C with 5% CO_2. Human keratinocyte (HaCaT) and bronchial epithelial (BEAS-2B) cell lines, acquired from the ATCC (Manassas, VA, USA), were maintained under conditions recommended by the suppliers: HaCaT cells in DMEM with 10% FBS and 1% penicillin-streptomycin, and BEAS-2B cells in airway epithelial basal medium with the bronchial epithelial growth kit (Lonza, Basel, Switzerland). All cultures were routinely screened for Mycoplasma contamination using the MycoAlert Mycoplasma Detection Kit (Lonza).

PBMC transfection

PBMCs were seeded in 6-well plates at a density of 2×10^6 cells per well. Reverse transfections were performed using HiPerFect (QIAGEN, Hilden, Germany), following the manufacturer's instructions. The following oligonucleotides were used: 5 nM miR-4717–3p mimic (QIAGEN, cat. no. 339173), 60 nM inhibitor (IDT, cat. no. 232724697), 7.5 nM PD-1-specific miR-4717–3p target site blocker (TSB) (QIAGEN, cat. no. 339194, sequence: AGGGTGGGCACATGGGG), and corresponding negative controls (mimic, NC1 inhibitor, negative TSB: ACGTCTATACGCCCA, QIAGEN). Forty-eight hours post-transfection, PBMCs were treated with 100 ng/mL interferon-gamma (IFN-γ, PeproTech EC, London, UK) for an additional 48 hours. Functional assays for RNA and protein analyses were conducted at 24 and 48 hours post-transfection, respectively.

RNA extraction and quantitative PCR

Total RNA, including miRNAs, was extracted 24 hours after transfection using the miRNeasy Mini Kit (QIAGEN, cat. no. 217004). RNA concentration and quality were determined with a NanoDrop spectrophotometer (Thermo Scientific). Ten nanograms of RNA were reverse-transcribed with the miRNA LNA PCR Starter Kit (QIAGEN, cat. no. 3616517), using U6 as an internal control. miR-4717–3p levels were normalized to miR103a-3p and quantified using the $2^{-\Delta\Delta CT}$ method. Total RNA was also isolated with TRIzol (Thermo Fisher, Waltham, MA, USA) and converted to cDNA using the SensiFAST cDNA Synthesis Kit (Bioline). PD-1 mRNA levels were assessed via qRT-PCR using SensiFAST SYBR No-ROX Kit (Bioline) on a LightCycler 480 II (Roche, Basel, Switzerland), with GAPDH as a housekeeping gene. Primer sequences were: PD-1 forward: CGTGGCCTATCCACTCCTCA, reverse: ATCCCTTGTCCCAGCCACTC; GAPDH forward: CTGACTTCAACAGCGACACC, reverse: TAGCCAAATTCGTTGTCATACC. Relative expression was calculated with the $2^{-}\Delta\Delta Cq$ method [37]. All assays were performed in triplicate across three independent experiments.

Western blotting

Forty-eight hours after transfection, PBMCs were harvested and lysed as previously described [38]. Protein extracts were subjected to western blotting using antibodies against PD-1 (Cell Signaling, cat. no. 86163), GAPDH (Cell Signaling, cat. no. 5174), and horseradish peroxidase-conjugated secondary antibodies (Cell Signaling, cat. no. 7074). GAPDH served as a loading control. Experiments were conducted in triplicate.

Flow cytometry

PBMCs (2×10^6 cells/well) were treated with 100 ng/mL IFN-γ for 48 hours, with untreated cells as controls. Cells were stained with PE-conjugated anti-PD-1 antibody (BioLegend, cat. no. 329905), using PE anti-mouse IgG1k (BioLegend, cat. no. 406607) as specificity control. Staining was performed as described [35], and samples were analyzed using a FACSVerse flow cytometer (BD Biosciences, Swindon, UK). Mean fluorescence intensity was calculated from three independent experiments.

HLA class I genotyping

Genotyping of HLA class I alleles was performed at the Transplant Hematological Unit, "San Giovanni di Dio e Ruggi D'Aragona" University Hospital, as described [39], and validated using the TRON Cell Line Portal (https://www.cellosaurus.org/CVCL_0038).

Co-culture with non-cancer cell lines

PBMCs from six patients were selected for co-culture based on tumor type, clinical response to ICI therapy, rs10204525 genotype (C/C or C/T), and HLA compatibility with HaCaT or BEAS-2B cells. Transfected and untransfected PBMCs were added to HaCaT or BEAS-2B cells (2×10^5 cells/well, 5:1 effector-to-target ratio) in 24-well plates and incubated with 10 µg/mL nivolumab ± 3.3 µg/mL ipilimumab for 24 or 48 hours, reflecting the 3:1 mass ratio used in clinical trials CheckMate 012 and 9LA [14, 40]. Human IgG4 and IgG were used as isotype controls, and monocultured HaCaT or BEAS-2B cells served as additional controls.

Assessment of cell viability

After co-culture, HaCaT and BEAS-2B cells were washed with PBS and viability was determined using Cell Counting Kit-8 (Dojindo Laboratories, Rockville, MD, USA), with absorbance measured at 450 nm on a Sunrise microplate reader (TECAN, Männedorf, Switzerland). Experiments were performed in triplicate and repeated 3 times.

Measurement of IFN-γ secretion

Supernatants from co-cultured cells were collected at 24 and 48 hours and analyzed for interferon-gamma (IFN-γ) content using the Human IFN-γ ELISA Max Deluxe Set (BioLegend) according to the manufacturer's instructions. Absorbance was read at 450 nm on a Sunrise microplate reader (TECAN, Männedorf, Switzerland). Each experiment was performed in triplicate and repeated in three independent sessions.

Assessment of apoptosis in co-cultured cells

HaCaT and BEAS-2B cells were washed with PBS following 24 or 48 hours of co-culture and subjected to apoptosis detection using Annexin V-FITC and propidium iodide (PI) staining (Annexin V-FITC Early Apoptosis Detection Kit, Cell Signaling Technology) to discriminate viable, early apoptotic, and necrotic populations, as per the manufacturer's protocol. Flow cytometric analysis was conducted on a FACSVerse cytometer (BD Biosciences), and results reflect three independent experiments.

Data processing and statistical methodology

All datasets were initially compiled in Microsoft Excel and analyzed using Stata V.13 (StataCorp LP, College Station, TX, USA) and GraphPad Prism V.6.0 (GraphPad Software, La Jolla, CA, USA). Continuous variables were summarized as medians with ranges, whereas categorical variables were expressed as counts and percentages. Kaplan-Meier curves were used to estimate progression-free survival (PFS) and overall survival (OS). Associations between PD-1 SNPs and clinical-pathological parameters, objective response rate (ORR), and immune-related adverse events (irAEs) were assessed using Fisher's exact test, Mann-Whitney U test, or Kruskal-Wallis test, as appropriate. Log-rank tests were applied to examine the effect of PD-1 SNPs, clinical variables, and irAEs on PFS and OS. Comparisons between groups were performed using two-sided unpaired t-tests or one-way ANOVA, and p-values <0.05 were considered statistically significant.

Clinical and pathological characteristics of the anti-PD-1/PD-L1 cohort

The first patient cohort consisted of 72 Caucasian individuals with advanced malignancies treated at "San

Giovanni di Dio e Ruggi D'Aragona" University Hospital. The distribution of tumor types included 49 cases of NSCLC (68.1%), 9 cases of RCC (12.5%), 8 cases of HNSCC (11.1%), and 6 cases of melanoma (8.3%). Comprehensive baseline clinical and pathological characteristics are summarized in **Table 1**.

Table 1. Baseline clinical and pathological characteristics of patients in the first cohort

Characteristic	Value
Median age	66 years (range 43–84)
Sex	Male: 59 (81.9%) Female: 13 (18.1%)
ECOG performance status	0: 26 (36.1%) 1: 28 (38.9%) 2: 18 (25.0%)
Smoking history	Never smoked: 13 (18.1%) Former smoker: 44 (61.1%) Current smoker: 15 (20.8%)
Comorbid conditions	Hypertension: 43 (59.7%) Dyslipidemia: 19 (26.4%) Diabetes: 14 (19.4%) COPD: 8 (11.1%) Heart failure: 6 (8.3%) Chronic renal failure: 0 (0.0%) Immune disorders: 0 (0.0%)
Cancer type	NSCLC: 49 (68.1%) RCC: 9 (12.5%) HNSCC: 8 (11.1%) Melanoma: 6 (8.3%)
Asymptomatic brain metastases	Yes: 14 (19.4%) No: 58 (80.6%)
Line of treatment	First-line: 11 (15.3%) Second-line: 61 (84.7%)
Prior chemotherapy	Yes: 51 (70.8%) No: 21 (29.2%)
Previous targeted therapy	Yes: 10 (13.9%) No: 62 (86.1%)
Type of monoclonal antibody	Nivolumab: 55 (76.4%) Pembrolizumab: 9 (12.5%) Atezolizumab: 8 (11.1%)
Median number of anti-PD-1/PD-L1 therapy cycles	8 (range 1–83)
Response to therapy	Complete response (CR): 4 (5.6%) Partial response (PR): 16 (22.2%) Stable disease (SD): 12 (16.7%) Progressive disease (PD): 40 (55.6%) Objective response rate (ORR): 20 (29.4%)
Survival outcomes	Median follow-up: 21.93 months (range 5.53–46.67) Median PFS: 4.15 months (range 0.46–46.67) Median OS: 10.70 months (range 0.46–46.67)

Abbreviations: COPD= chronic obstructive pulmonary disease; CR= complete response; ECOG PS= Eastern Cooperative Oncology Group performance status; HNSCC= head and neck squamous cell carcinoma; mAb= monoclonal antibody; NSCLC= non-small cell lung cancer; ORR= objective response rate; OS= overall survival; PD= progressive disease; PD-1= programmed cell death-1; PD-L1= programmed cell death ligand 1; PFS, progression-free survival; PR= partial response; RCC= renal cell carcinoma; SD= stable disease.

The study cohort had a median age of 66 years, ranging from 43 to 84 years. The majority of patients were male (59, 81.9%). Regarding performance status, 54 patients (75.0%) had an ECOG PS of 0–1, while 18 (25.0%) had a score of 2. In terms of smoking history, 13 patients (18.1%) had never smoked, 44 (61.1%) were former smokers, and 15 (20.8%) were current smokers. Common comorbid conditions included hypertension (43, 59.7%), dyslipidemia (19, 26.4%), diabetes (14, 19.4%), chronic obstructive pulmonary disease (8, 11.1%), and heart failure (6, 8.3%). Asymptomatic brain metastases were observed in 14 patients (19.4%). Most individuals (84.7%) received anti-PD-1/PD-L1 therapy as a second-line treatment. Prior therapies included chemotherapy in 51 patients (70.8%) and targeted therapy in 10 patients (13.9%). Overall, 88.9% of patients were treated with anti-PD-1 antibodies and 11.1% with anti-PD-L1 antibodies; specifically, 55 patients (76.4%) received nivolumab, 9 (12.5%) received pembrolizumab, and 8 (11.1%) received atezolizumab. The objective response rate (ORR) was 27.8%, with complete responses (CR) in 4 patients (5.6%), partial responses (PR) in 16 patients (22.2%), stable disease (SD) in 12 patients (16.7%), and progressive disease (PD) in 40 patients (55.6%). At a median follow-up of 21.93 months (range, 5.53–46.67), 21 of 72 patients (29.2%) remained alive. Median progression-free survival (PFS) and overall survival (OS) were 4.15 months (range, 0.46–46.67) and 10.70 months (range, 0.46–46.67), respectively **(Figure 1)**.

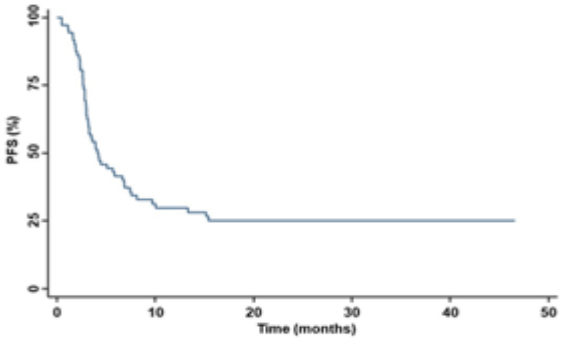

a)

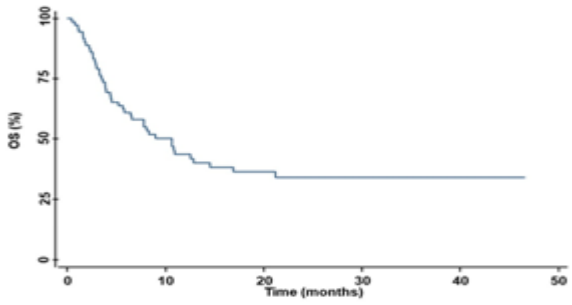

b)

Figure 1. Progression-free and overall survival in patients with advanced malignancies treated with anti-PD-1/PD-L1 monoclonal antibodies. Kaplan-Meier analysis was used to evaluate progression-free survival (PFS) and overall survival (OS) in patients receiving atezolizumab, nivolumab, or pembrolizumab. At a median follow-up of 21.93 months (range, 5.53–46.67 months), the median PFS was 4.15 months (panel a), and the median OS was 10.70 months (panel b). Abbreviations: mAbs=monoclonal antibodies; PD-1= programmed cell death-1; PD-L1= programmed cell death ligand 1; PFS= progression-free survival; OS, overall survival.

Treatment-related adverse events of grades 1–2 and 3–4 were observed in 45 patients (62.5%) and 6 patients (8.3%), respectively **(Table 2)**.

Table 2. Rates of immune-related adverse events (irAEs) in the first cohort

Adverse Event	Grade 3–4, n (%)	Grade 1–2, n (%)
Any event	6 (8.33%)	45 (62.50%)
Led to treatment discontinuation	3 (4.17%)	0 (0.00%)
Adrenal insufficiency	0 (0.00%)	8 (11.11%)
Amylase increase	0 (0.00%)	2 (2.78%)
Arthritis	0 (0.00%)	3 (4.17%)
Asthenia	0 (0.00%)	23 (31.94%)
Alanine aminotransferase increase	1 (1.39%)	1 (1.39%)
Aspartate aminotransferase increase	1 (1.39%)	3 (4.17%)
Colitis	0 (0.00%)	2 (2.78%)
Creatinine increase	0 (0.00%)	7 (9.72%)
Decreased appetite	2 (2.78%)	5 (6.94%)
Diarrhea	0 (0.00%)	7 (9.72%)
Fever	0 (0.00%)	8 (11.11%)
Gynecomastia	0 (0.00%)	1 (1.39%)
Hypophysitis	0 (0.00%)	1 (1.39%)
Lipase increase	1 (1.39%)	3 (4.17%)
Nausea	3 (4.17%)	4 (5.56%)
Oral mucositis	0 (0.00%)	3 (4.17%)
Pancreatitis	2 (2.78%)	1 (1.39%)
Pneumonitis	1 (1.39%)	2 (2.78%)
Pruritus	0 (0.00%)	9 (12.50%)
Rash	1 (1.39%)	4 (5.56%)
Thyroiditis	0 (0.00%)	18 (25.00%)
Vitiligo	0 (0.00%)	1 (1.39%)
Vomiting	0 (0.00%)	5 (6.94%)

Abbreviation: irAE, immune-related adverse event.

Among the immune-related adverse events, the most commonly observed grade 1–2 event was asthenia, affecting 31.94% of patients, whereas nausea was the most frequent grade 3–4 event, occurring in 4.17% of

cases. Three patients (4.17%) discontinued anti-PD-1/PD-L1 therapy due to irAEs, and no deaths related to treatment were recorded.

Genotyping and characterization of PD-1 SNPs in patients undergoing anti-PD-1/PD-L1 therapy

The study population was genotyped for six PD-1 single nucleotide polymorphisms: rs2227982, rs36084323, rs11568821, rs7421861, rs2227981, and rs10204525. The distribution and frequency of these PD-1 SNPs are summarized in **Table 3**.

Table 3. Distribution of PD-1 SNP genotypes in the study cohort

SNP	Location	Genotype	Frequency, n (%)
rs2227982	Exon	G/G	69 (95.83)
		G/A	3 (4.17)
		A/A	0 (0.00)
rs36084323	Promoter region	C/C	69 (95.83)
		C/T	3 (4.17)
		T/T	0 (0.00)
rs11568821	Intron	C/C	58 (80.56)
		C/T	13 (18.06)
		T/T	1 (1.39)
rs7421861	Intron	A/A	41 (56.94)
		A/G	26 (36.11)
		G/G	5 (6.94)
rs2227981	Exon	G/G	11 (25.00)
		A/G	21 (47.73)
		A/A	12 (27.27)
rs10204525	3'-UTR	C/C	60 (83.33)
		C/T	12 (16.67)
		T/T	0 (0.00)

Abbreviations: PD-1= programmed cell death-1; SNP= single nucleotide polymorphism; 3'-UTR= 3′ untranslated region.

Analysis of the genomic locations of the PD-1 SNPs revealed that rs2227982 and rs2227981 are situated in exonic regions (chr2:241,851,281 and chr2:241,851,121, respectively), whereas rs11568821 and rs7421861 are located within introns (chr2:241,851,760 and chr2:241,853,198, respectively). The rs36084323 SNP maps to the promoter region (chr2:241,859,444), and rs10204525 is positioned in the 3'-UTR (chr2:241,850,169).

Associations between clinical-pathological characteristics, outcomes, irAEs, and PD-1 SNPs

No statistically significant correlations were observed between clinical-pathological characteristics, treatment outcomes, and the occurrence of irAEs. Similarly, clinical features and outcomes showed no significant association with any of the analyzed PD-1 SNPs. Moreover, no meaningful relationships were detected between PD-1 SNPs rs2227981, rs7421861, rs11568821, rs36084323, rs2227982 and the development of irAEs. In contrast, rs10204525 genotypes were significantly linked to irAE incidence: patients with the C/C genotype experienced higher rates of both grade 1–2 ($p = 0.0053$) and grade 3–4 irAEs ($p < 0.0001$) compared with carriers of the C/T genotype. Notably, no grade 3–4 irAEs were reported in C/T carriers, and they also lacked grade 1–2 irAEs of particular concern, including arthritis, ALT/AST elevation, pancreatitis, nausea, or adrenal insufficiency.

To confirm these findings, the predictive impact of rs10204525 was further evaluated in a cohort of 27 patients with advanced, non-oncogene-addicted NSCLC receiving first-line therapy with either PBCT plus pembrolizumab or PBCT combined with nivolumab and ipilimumab between April 2021 and May 2024. In this cohort, grade 1–2 and grade 3–4 irAEs occurred in 18 (66.67 percent) and 9 (33.33 percent) patients, respectively. Asthenia (33.33 percent) and pneumonitis (14.81%) were the most commonly reported grade 1–2 and grade 3–4 irAEs, respectively. Five patients (18.52%) discontinued combination therapy due to irAEs, and no treatment-related deaths were recorded. The rs10204525 PD-1 SNP was distributed as C/C in 18 patients (66.67%), C/T in 9 patients (33.33%), and T/T in none (0.00%). Consistent with the previous cohort, patients with the C/C genotype experienced significantly higher rates of grade 1–2 ($p = 0.0012$) and grade 3–4 irAEs ($p = 0.0116$) compared with C/T carriers, and no grade 3–4 irAEs occurred in C/T genotype carriers.

Identification of candidate miRNAs targeting rs10204525 in the PD-1 3'-UTR

Since rs10204525 is located in the 3'-UTR of PD-1, its allelic variants could influence the binding of specific miRNAs, thereby modulating PD-1 expression. To investigate this, potential miRNAs interacting with rs10204525 based on allele specificity were identified using the miRNASNP-v4 database. Four miRNAs—miR-3945-942-3p, miR-4717-3p, miR-5589-3p, and

miR-4802-3p—were predicted to bind to rs10204525 in an allele-dependent manner **(Table 4)**.

Table 4. Predicted miRNAs binding to rs10204525 in the PD-1 3′-UTR based on ΔMFE between C and T alleles

Putative miRNA	Seed region	Length (nt)	ΔMFE (kcal/mol)
miR-942–3p	7	21	−12.8
miR-4717–3p	8	20	−26.70
miR-3115–5589–3p	8	22	−20.60
miR-4802–3p	7	22	−13.70

Abbreviations: miRNA= microRNA; PD-1= programmed cell death-1; 3'-UTR= 3′ untranslated region; ΔMFE= differential minimum free energy of hybridization.

All four identified miRNAs were predicted to recognize a seed region of 7–8 nucleotides that included the critical rs10204525 locus; however, miR-4717–3p exhibited the most favorable thermodynamic profile, as reflected by the lowest ΔMFE, indicating the strongest predicted miRNA:mRNA binding affinity. Consequently, miR-4717–3p was selected for further functional investigation to evaluate its potential role in modulating PD-1 expression through allele-specific binding to rs10204525.

To explore this, PBMCs carrying either the C/C ($PBMCs^{C/C}$) or C/T ($PBMCs^{C/T}$) genotypes at rs10204525 were isolated from patient blood samples, cultured, and subjected to transfection with (1) a specific miR-4717–3p mimic, (2) a specific miR-4717–3p inhibitor, or (3) a target site blocker (TSB). Control experiments using a negative miRNA mimic, negative miRNA mimic plus negative TSB, and negative inhibitor did not alter miR-4717–3p levels, establishing the negative miRNA mimic as the appropriate control for subsequent analyses. The efficiency of miRNA transfection was confirmed by measuring miR-4717–3p levels under basal conditions and after IFN-γ stimulation **(Figure 2a)** [41]. Specifically, miR-4717–3p levels were elevated following transfection with the mimic, with or without TSB, and were reduced following inhibitor transfection, independent of rs10204525 genotype. IFN-γ incubation, used to mimic PBMC activation and induce PD-1 upregulation [41], did not modify miR-4717–3p expression under any transfection condition in either $PBMCs^{C/C}$ or $PBMCs^{C/T}$.

Assessment of PD-1 expression at both mRNA and protein levels, under basal conditions and after IFN-γ exposure, demonstrated that miR-4717–3p differentially regulated PD-1 depending on the rs10204525 genotype **(Figures 2b–2d)**. At baseline, PD-1 expression was higher in $PBMCs^{C/T}$ transfected with negative miRNA mimic compared with $PBMCs^{C/C}$. In $PBMCs^{C/C}$, miR-4717–3p mimic significantly suppressed PD-1 levels, whereas the inhibitor increased them; these effects were not observed in $PBMCs^{C/T}$. Similarly, TSB alone upregulated PD-1 expression in $PBMCs^{C/C}$ but had no effect in $PBMCs^{C/T}$. IFN-γ stimulation increased PD-1 expression across all conditions regardless of genotype or miR-4717–3p modulation; however, the magnitude of PD-1 induction was greater in $PBMCs^{C/T}$ than in $PBMCs^{C/C}$.

These findings confirm a causal relationship between the allele-specific binding of miR-4717–3p and PD-1 regulation, demonstrating that miR-4717–3p negatively controls PD-1 expression and induction only in the presence of the C/C genotype at rs10204525, whereas this regulatory effect is lost in C/T carriers.

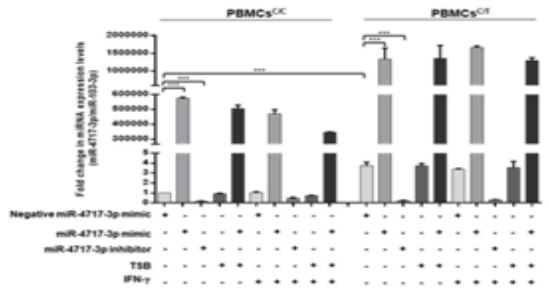

a)

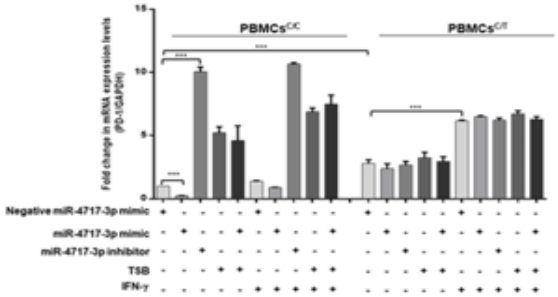

b)

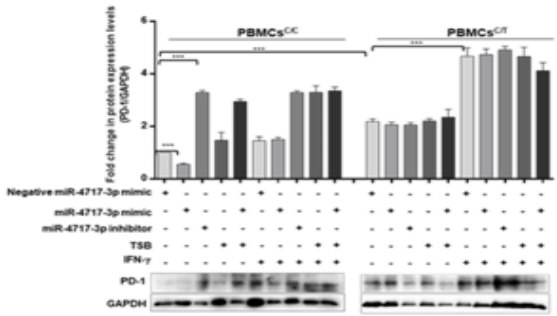

c)

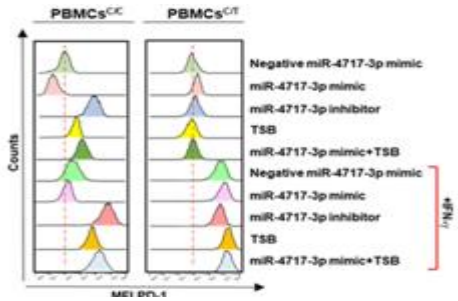

d)

Figure 2. Regulation of PD-1 expression by miR-4717–3p according to the rs10204525 genotype in human PBMCs under both basal conditions and after IFN-γ stimulation. PBMCs^C/C and PBMCs^C/T were transfected for 48 hours with either a miR-4717–3p mimic, inhibitor, TSB, or a combination of the mimic with TSB, with a negative miRNA mimic serving as control. Transfected PBMCs were then seeded into 24-well plates at 2×10^5 cells per well and incubated with IFN-γ (100 ng/mL). After 24 hours at 37°C in 5% CO2, miR-4717–3p expression, normalized to miR-103–3p, and PD-1 mRNA levels, normalized to GAPDH, were measured by RT-PCR (a and b). Data were expressed as mean ± SD of three independent experiments, comparing each treatment to the negative mimic control (***p≤0.001). Following 48 hours of incubation, PBMCs were lysed and PD-1 protein expression was assessed by western blot using PD-1-specific antibodies, with GAPDH as a loading control (c). Quantified results were plotted as mean ± SD of three independent experiments (***p≤0.001). Additionally, cell surface PD-1 expression was evaluated by staining with PE-conjugated anti-PD-1 antibody and analyzed by flow cytometry; PE anti-mouse IgG1k was used as a specificity control (d). Representative histograms of MFI-PD-1 are shown from three independent experiments. Abbreviations: Ab= antibody; IFN= interferon; MFI= mean fluorescence intensity; mRNA= messenger RNA; PBMC= peripheral blood mononuclear cell; PD-1= programmed cell death-1; PE= phycoerythrin; RT-PCR, real-time PCR; TSB= target site blocker.

To determine the functional consequences of allele-specific miR-4717–3p modulation of PD-1 expression on immune reactivity, we performed co-culture experiments using non-cancer HaCaT cells with HLA class I-matched $PBMCs^{C/C}$ and $PBMCs^{C/T}$, either under basal conditions or after incubation with anti-PD-1 nivolumab **(Figure 3)**. HLA class I typing revealed that HaCaT cells were homozygous for HLA-A31:01 and heterozygous for HLA-B40:01:02, 51:01:01 and HLA-C03:04:01, 15:02:01. PBMCs were obtained from two patients (Patient #1 and #2) selected based on comparable clinical-pathological features, distinct rs10204525 genotypes, and HLA compatibility with HaCaT cells ($PBMC^{C/C}$ matched for HLA-A31:01 and HLA-C03:04:01; $PBM^{CC/T}$ matched for HLA-A02:01). Notably, both patients had advanced NSCLC and were long-term responders to second-line anti-PD-1 therapy; one developed irAEs with the C/C genotype, while the other, carrying the C/T genotype, did not **(Table 5)**.

Table 5. Clinical-pathological characteristics of NSCLC patients selected for PBMC co-culture experiments

	Patient #6	Patient #5	Patient #4	Patient #3	Patient #2	Patient #1
rs10204525 genotype	C/T	C/C	C/T	C/C	C/T	C/C
HLA-A	A01:01/A02:01	A24:01/A03:01	A02:01/A31:01	A24:02/A31:01	A02:01/A11:01	A02:01/A31:01
HLA-B	B08:01/B15:01	B07:02/B51:01	B15:01/B40:01	B08:01/B51:01	B15:01/B40:01	B07:02/B08:01
HLA-C	C03:04/C07:01	C07:01/C15:02	C03:04/C07:01	C07:02/C15:02	C03:04/C15:02	C03:04/C07:02
ECOG PS	0	0	0	1	0	0
Smoking status	Current smoker	Former smoker	Former smoker	Current smoker	Former smoker	Former smoker

Comorbidities	None	Hypertension, Dyslipidemia	Hypertension	None	Hypertension	Hypertension
Histology	Adenocarcinoma	Adenocarcinoma	Adenocarcinoma	Adenocarcinoma	Adenocarcinoma	Adenocarcinoma
Asymptomatic brain metastases	No	No	No	No	No	No
Previous PBCT	No	Yes	Yes	Yes	Yes	Yes
Previous targeted therapy	No	No	No	No	No	No
Type of ICI-based immunotherapy	PBCT + Nivolumab + Ipilimumab	PBCT + Nivolumab + Ipilimumab	Nivolumab	Nivolumab	Nivolumab	Nivolumab
Number of ICI-based therapy cycles	14	3	38	50	40	45
Best response	CR	PR	PR	PR	PR	PR
Grade 1–2 irAEs	ASTH, ALT/AST inc., Amylase/Lipase inc., Oral mucositis	ALT/AST inc.	ASTH	ASTH, Nausea, Thyroiditis	None	ASTH, Creatinine inc., Lipase inc.
Grade 3–4 irAEs	None	*ALT/AST inc.	None	Rash	None	None

*Led to discontinuation of ICI-based immunotherapy.CR= complete response; ECOG PS= Eastern Cooperative Oncology Group performance status; HLA= human leukocyte antigen; ICI= immune checkpoint inhibitor; irAE= immune-related adverse event; NSCLC, non-small cell lung cancer; PBCT= platinum-based chemotherapy; PBMC= peripheral blood mononuclear cell; PR= partial response.

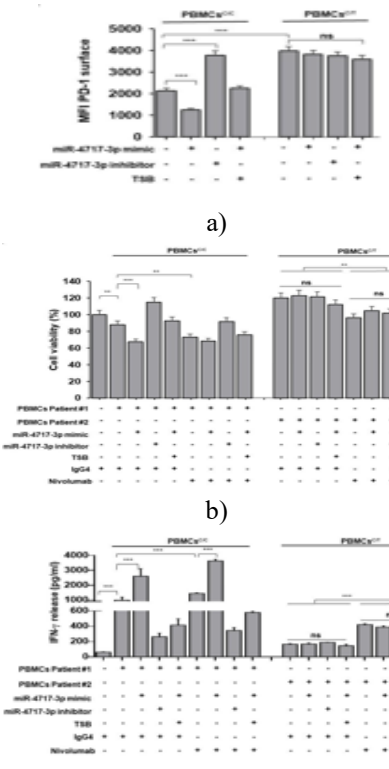

a) b) c)

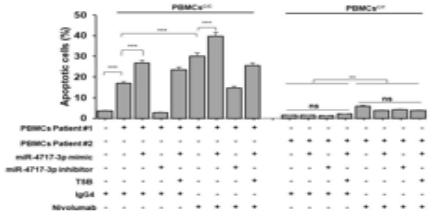

d)

Figure 3. Allele-specific modulation by rs10204525 of in vitro anti-PD-1 nivolumab activity on transfected PBMCs co-cultured with HLA-matched HaCaT cells. HaCaT cells were plated in 24-well plates at a density of 2×10^5 cells per well and incubated for 48 hours at 37°C with 5% CO_2. Subsequently, HLA-matched PBMCs (C/C and C/T) isolated from Patient #1 and #2 and transfected with miRNA-specific constructs (miR-4717–3p mimic, inhibitor, or a combination of mimic and TSB) were added in a 1:5 ratio, followed by treatment with 10 µg/mL anti-PD-1 nivolumab or human IgG4 isotype control for 24 hours. Negative miRNA mimic-transfected PBMCs served as controls. (a) Forty-eight hours post-transfection, PBMCs were harvested and surface-stained with PE-conjugated anti-PD-1

IgG1k antibody; PE anti-mouse IgG1k served as a specificity control. Data, expressed as mean fluorescence intensity (MFI), represent three independent experiments. (b) HaCaT cell viability was assessed via CCK-8 assay, expressed as mean ± SD relative to HaCaT cells cultured alone, with results from three independent experiments, each performed in triplicate. (c) IFN-γ levels in the culture supernatant were measured using ELISA, reported as mean ± SD from three independent experiments in triplicate. (d) Apoptosis in HaCaT cells was determined by annexin V/PI flow cytometry, with results expressed as mean ± SD of annexin V^+ cells from three independent experiments. Statistical significance: *p<0.05; **p<0.01; ***p<0.001; ns = not significant. Abbreviations: Ab, antibody; CCK-8, cell counting kit-8; HaCaT, human epidermal keratinocyte; IFN, interferon; MFI, mean fluorescence intensity; PBMC, peripheral blood mononuclear cell; PD-1, programmed cell death-1; PE, phycoerythrin; PI, propidium iodide; TSB, target site blocker.

Quantification of PD-1 surface expression on PBMCs under all experimental conditions confirmed efficient miR-4717–3p modulation **(Figure 3a)**. Consistent with prior findings, transfection of PBMCsC/C with miR-4717–3p mimic significantly reduced PD-1 surface expression, whereas transfection with miR-4717–3p inhibitor or mimic plus TSB increased PD-1 levels. Conversely, in PBMCsC/T, PD-1 expression remained unchanged regardless of miR-4717–3p modulation. Co-culture with PBMCsC/C resulted in higher HaCaT cell growth inhibition, apoptosis induction, and IFN-γ release compared with PBMCsC/T **(Figures 3b–3d)**. Moreover, transfection of PBMCsC/C with miR-4717–3p mimic or inhibitor significantly reduced growth inhibition and apoptosis induction in HaCaT cells, while IFN-γ release was not substantially altered, relative to negative miRNA mimic-transfected PBMCsC/C. Similar results were observed when PBMCsC/C were transfected with the combination of miR-4717–3p mimic and TSB. In contrast, HaCaT cells co-cultured with miR-4717–3p-modulated PBMCsC/T showed no significant changes in growth inhibition, apoptosis, or IFN-γ release compared with controls. Treatment with nivolumab enhanced PBMC-mediated HaCaT cell killing and IFN-γ production in a genotype-dependent manner: in PBMCsC/C, nivolumab significantly increased growth inhibition, apoptosis, and IFN-γ release in negative miRNA mimic-transfected cells and further amplified these effects in miR-4717–3p mimic-transfected PBMCsC/C **(Figures 3b–3d)**. By contrast, nivolumab had minimal effects on PBMCsC/T, with only slight decreases in HaCaT viability and modest increases in IFN-γ production and apoptosis **(Figures 3b–3d)**.

Validation of rs10204525 genotype-dependent PBMC reactivity toward non-cancer cells with anti-PD-1 alone or combined with anti-CTLA-4 mAb. To corroborate clinical and in vitro findings, BEAS-2B and HaCaT cells were co-cultured with additional HLA class I-matched PBMCsC/C and PBMCsC/T under basal conditions or after treatment with nivolumab **(Figure 4)** or nivolumab plus ipilimumab **(Figure 5)**. BEAS-2B cells were homozygous for HLA-A02:01 and HLA-C07:01 and heterozygous for HLA-B*07:02/15:01. PBMCs were collected from four additional patients (#3–6; **(Table 5)**), all with advanced NSCLC and clinical benefit from anti-PD-1 therapy. Patients #3–4 received nivolumab as second-line therapy, while #5–6 received first-line PBCT plus nivolumab and ipilimumab. All C/C carriers developed grade 3–4 immune-related adverse events (irAEs), while C/T carriers did not; C/C patients also experienced more grade 1–2 irAEs, with grade 3–4 events leading to therapy discontinuation in patient #5. Analyses of HaCaT and BEAS-2B cell growth inhibition, apoptosis, and IFN-γ release confirmed that PBMCsC/C exhibited significantly heightened reactivity toward non-cancer cells upon anti-PD-1 treatment alone **(Figure 4)** or combined with anti-CTLA-4 **(Figure 5)** compared with PBMCsC/T. Anti-CTLA-4 treatment further potentiated anti-PD-1-mediated susceptibility, particularly in PBMCsC/C.

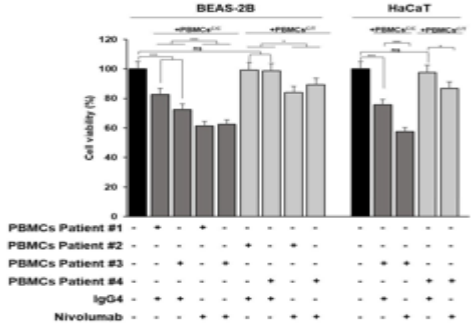

a)

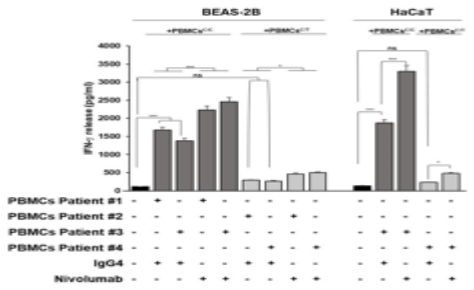

b)

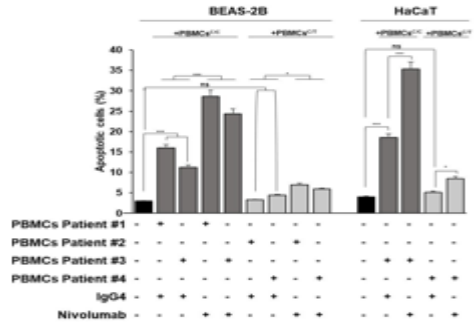

c)

Figure 4. rs10204525 genotype-dependent differences in PBMC-mediated immune responses toward non-cancer cells under anti-PD-1 treatment in NSCLC patients. HaCaT and BEAS-2B cells were plated in 24-well plates at 2×10^5 cells per well and incubated for 24 hours at 37°C with 5% CO_2. Cells were then co-cultured with HLA-matched PBMCsC/C and PBMCsC/T isolated from Patients #1–4 at a 1:5 ratio, followed by treatment with 10 µg/mL anti-PD-1 nivolumab or human IgG4 isotype control for forty eight hours. Monocultured HaCaT and BEAS-2B cells served as controls. (a) Cell viability of non-cancer cells after 48 hours was assessed using the CCK-8 assay, and data are expressed as mean ± SD relative to monocultured cells, based on three independent experiments, each performed in triplicate. (b) IFN-γ levels in culture supernatants were quantified using the ELISA Max Deluxe Set Human IFN-γ kit and are reported as mean ± SD from three independent experiments in triplicate. (c) Apoptosis in HaCaT and BEAS-2B cells was evaluated by annexin V/PI flow cytometry, with results expressed as mean ± SD of annexin V^+ cells from three independent experiments. Statistical significance: *p<0.05; **p<0.01; ***p<0.001; ns = not significant. Abbreviations: BEAS-2B, bronchial epithelial cells; CCK-8= cell counting kit-8; HaCaT= human epidermal keratinocytes; IFN= interferon; NSCLC= non-small cell lung cancer; PBMC= peripheral blood mononuclear cells; PD-1= programmed cell death-1; PI= propidium iodide.

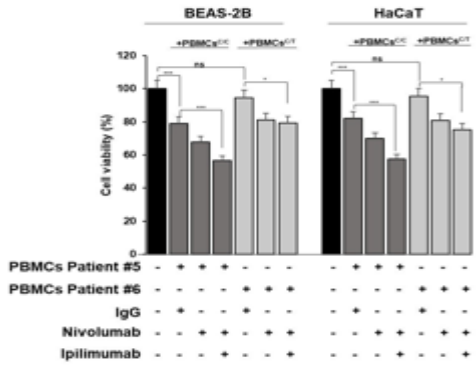

a)

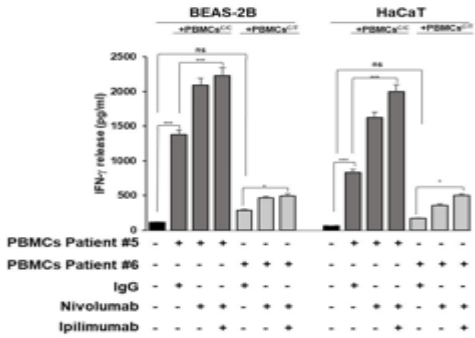

b)

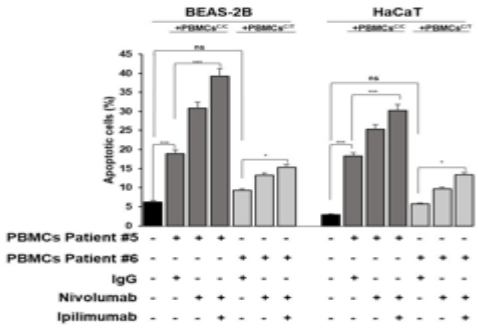

c)

Figure 5. Enhanced immune response in rs10204525 C/C PBMCs from NSCLC patients under anti-PD-1 or combined anti-PD-1/CTLA-4 treatment in co-culture with non-cancer cells. HaCaT and BEAS-2B cells were seeded in 24-well plates at 2×10^5 cells per well and incubated for 24 hours at 37°C with 5% CO_2. Cells were then co-cultured with HLA-matched PBMCsC/C and PBMCsC/T isolated from Patients #5 and #6 at a 1:5 ratio and treated with 10 µg/mL anti-PD-1 nivolumab alone or combined with 3.3 µg/mL anti-CTLA-4 ipilimumab for 48 hours. Human IgG was used as an isotype control, and

monocultured HaCaT and BEAS-2B cells served as controls. (a) Cell viability after 48 hours was determined using the CCK-8 assay, with results expressed as mean ± SD relative to monocultured cells, based on three independent experiments performed in triplicate. (b) IFN-γ levels in culture supernatants were measured by ELISA Max Deluxe Set Human IFN-γ kit and reported as mean ± SD from three independent experiments in triplicate. (c) Apoptosis of HaCaT and BEAS-2B cells was assessed by annexin V/PI flow cytometry, with data expressed as mean ± SD of annexin V^+ cells from three independent experiments. Statistical significance: *p<0.05; **p<0.01; ***p<0.001; ns = not significant. Abbreviations: CCK-8= cell counting kit-8; CTLA-4= cytotoxic T-lymphocyte antigen 4; HaCaT= human epidermal keratinocyte; IFN= interferon; NSCLC= non-small cell lung cancer; PBMC= peripheral blood mononuclear cells; PD-1= programmed cell death-1; PI= propidium iodide.

Results and Discussion

Anti-PD-1/PD-L1 immunotherapy has transformed the treatment of multiple cancer types, improving survival and quality of life compared with conventional therapies [1–11]. While generally well-tolerated, some patients develop severe immune-related adverse events (irAEs), which can cause lasting complications or be fatal [1–11]. The incidence of severe irAEs varies depending on the type of ICI therapy, ranging from 10% to 70%. In our study, two patient cohorts were included: the first consisted of advanced cancer patients receiving anti-PD-1/PD-L1 monotherapy, while the second included advanced NSCLC patients treated with anti-PD-1 plus platinum-based chemotherapy, with or without ipilimumab. The validity of these populations is supported by observed irAE rates, treatment discontinuations, and clinical outcomes (ORR and survival), which align with previously reported data for anti-PD-1/PD-L1 therapy [1–14].

Although several biomarkers have been explored to predict response to anti-PD-1/PD-L1 therapy, few studies have focused on identifying predictors of irAEs, and none have proven sufficiently reliable. Here, we validated a PD-1 single nucleotide polymorphism (SNP), rs10204525, which effectively predicts both grade 1–2 and grade 3–4 irAEs in patients undergoing anti-PD-1/PD-L1 therapy. Previous studies on the predictive value of PD-1 SNPs for irAEs have yielded conflicting results [42–46]. Our findings indicate that not all PD-1 SNPs are clinically relevant for irAE prediction; only rs10204525 was associated with irAE occurrence. Specifically, patients with the C/C genotype exhibited significantly higher rates of both grade 1–2 and grade 3–4 irAEs compared with those carrying the C/T genotype, regardless of whether they received anti-PD-1/PD-L1 alone or combined with chemotherapy and/or anti-CTLA-4 therapy.

These results are partially supported by Kobayashi *et al*., who reported that the G allele of rs10204525 is linked to increased risk of severe and multiple anti-PD-1-mediated irAEs [46], whereas Bins *et al*. and Refae *et al*. found no association [42, 44, 45]. In our first cohort, we included Caucasian patients with advanced cancers such as HNSCC, NSCLC, RCC, and melanoma treated with anti-PD-1/PD-L1 monotherapy in both first- and second-line settings. Variations in tumor types, patient ethnicity, and clinical-pathological characteristics may explain previously reported discrepancies. Importantly, our findings in a general cancer population were corroborated by a second cohort of advanced NSCLC patients receiving first-line anti-PD-1 therapy combined with chemotherapy, with or without anti-CTLA-4, reflecting real-world clinical practice. To our knowledge, no prior study has assessed the association between rs10204525 and irAEs in patients receiving anti-PD-1/PD-L1 combined with other oncologic treatments. Notably, three patients in the first cohort and five in the second cohort discontinued anti-PD-1/PD-L1 therapy due to severe irAEs, all of whom carried the C/C genotype.

Finally, the predictive value of rs10204525 for irAEs is reinforced by its known functional roles in autoimmunity, cancer susceptibility, and prognosis [26–31].

Conflicting evidence has also been reported regarding the relationship between irAE development and clinical response to ICIs in patients with solid tumors [47–49]. In our study, the occurrence of irAEs did not correlate with survival outcomes, and similarly, none of the analyzed PD-1 SNPs were associated with clinical survival. However, our conclusions are limited by the heterogeneity of tumor types, treatment lines, and the relatively small patient cohort. Additional studies are warranted to determine whether PD-1 SNPs and irAEs may influence overall survival in tumor-specific populations treated with ICIs.

The clinical significance of rs10204525 in predicting irAEs is further supported by the molecular mechanisms we delineate here for the first time. To our knowledge, no prior study has shown that rs10204525 predicts irAE development by mediating differential binding of miR-4717–3p to PD-1, thereby regulating its expression and induction. The causal link between miR-4717–3p and rs10204525 is demonstrated through differential modulation of miR-4717–3p in PBMCs from patients carrying distinct rs10204525 genotypes. In PBMCs with a C/C genotype, miR-4717–3p binds to the 3'-UTR of PD-1, resulting in PD-1 downregulation under both basal conditions and following IFN-γ stimulation, which induces PD-1 expression [41]. Conversely, in PBMCs with a C/T genotype, miR-4717–3p does not bind PD-1, leaving its expression and induction unaffected. Consequently, PBMCsC/T maintain higher PD-1 levels, serving as a regulatory mechanism for host immune responses [50].

The functional relevance of these allele-specific effects on PD-1 expression and irAE development was modeled by co-culturing normal keratinocytes and bronchial epithelial cells with patient-derived HLA-matched PBMCs carrying distinct rs10204525 genotypes. These experiments, which tested PBMC reactivity under anti-PD-1 or combined anti-PD-1/anti-CTLA-4 treatment, were designed to mimic irAE development. PBMCs with the C/C genotype exhibited reduced miR-4717–3p-mediated PD-1 expression and induction, which corresponded to enhanced recognition and cytotoxicity toward non-cancer cells, particularly under anti-PD-1 therapy. In contrast, PBMCs carrying the C/T genotype, with higher PD-1 expression due to lack of miR-4717–3p binding, displayed reduced reactivity toward non-cancer cells. These findings demonstrate that rs10204525 significantly modulates PD-1-mediated PBMC immunoreactivity **(Figure 6)**.

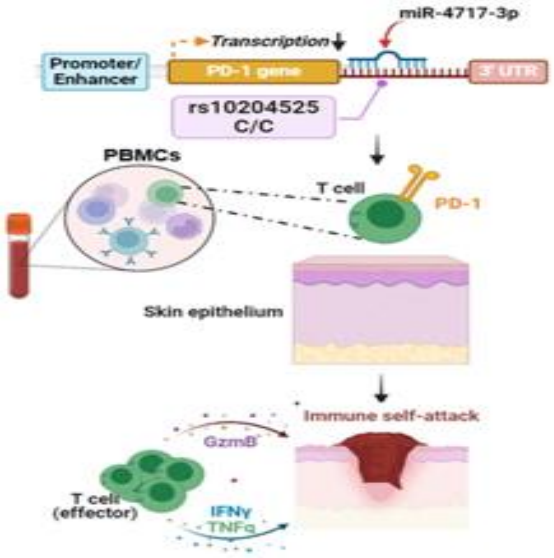

a)

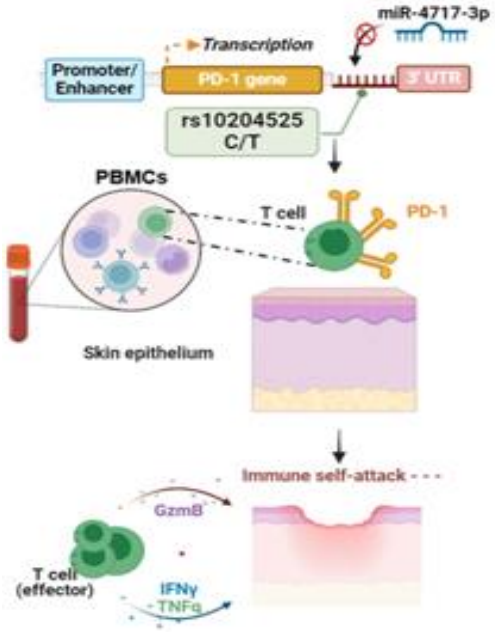

b)

Figure 6. Graphical summary of rs10204525 genotype influence on PD-1 expression and enhanced sensitivity of HaCaT cells to anti-PD-1 therapy. Abbreviations: 3'-UTR= 3′ untranslated region; GzmB= Granzyme B; HaCaT= human epidermal keratinocyte; IFN= interferon; PBMC= peripheral blood mononuclear cells; PD-1= programmed cell death-1; TNF= tumor necrosis factor.

Importantly, PBMCs used in the co-culture experiments were derived from advanced NSCLC patients who all experienced clinical benefit from anti-PD-1 therapy,

either alone or combined with chemotherapy and anti-CTLA-4. Patients with the C/C genotype exhibited a higher frequency and severity of irAEs compared with those carrying the C/T genotype. The selection of patients with comparable clinical-pathological characteristics and HLA class I matching to the non-cancer cell models ensures physiological relevance and robustness of the co-culture system, faithfully replicating immune interactions in a clinically meaningful HLA context. These findings highlight the clinical importance of genetic factors in determining the safety of anti-PD-1/PD-L1 immunotherapy, supporting a more personalized, risk-based approach to monitoring and managing potential irAEs. Furthermore, the lower susceptibility to irAEs observed in C/T carriers may indicate that this subgroup could tolerate more intensive or novel combinatorial ICI-based treatment strategies with reduced safety concerns.

Despite inclusion of a validation cohort, our study has limitations, including small sample sizes and tumor heterogeneity in the first cohort. Therefore, the influence of rs10204525 on irAE development should be confirmed in larger prospective studies. Additionally, most patients received either anti-PD-1 or anti-PD-L1 therapy, while only a small subset in the second cohort received a combination of platinum-based chemotherapy with anti-PD-1 and ipilimumab (anti-CTLA-4). Some evidence suggests that anti-PD-1 and anti-PD-L1 therapies may present different irAE profiles [51, 52]; however, in our study, no significant differences were observed between irAEs induced by anti-PD-1 versus anti-PD-L1. Consistent with previous reports [8, 12–14], combination therapies involving anti-PD-1 showed higher incidence and severity of irAEs compared with anti-PD-1/PD-L1 monotherapy. While we lacked sufficient power to compare irAE rates between patients receiving anti-PD-1 plus chemotherapy versus anti-PD-1 plus chemotherapy with anti-CTLA-4, our data show that anti-CTLA-4 increases PBMC-mediated susceptibility of non-cancer cells regardless of rs10204525 genotype, with a more pronounced effect in C/C carriers. Further studies are needed to determine whether rs10204525 differentially impacts irAE development in the context of diverse oncologic treatment combinations, including ICIs, chemotherapy, and targeted therapy. Additionally, mechanistic studies are warranted to elucidate the clinical significance of other PD-1 SNPs.

Conclusion

Overall, this study provides clinically relevant insights by identifying rs10204525 and miR-4717–3p-mediated modulation of PD-1 expression as a novel biomarker for predicting patients at higher risk of irAEs, while also illuminating a mechanism of immune cell reactivity. This biomarker may guide improved management and risk stratification for cancer patients undergoing anti-PD-1/PD-L1 therapy.

Acknowledgments: The authors wish to gratefully acknowledge the patients for participating in this study as well as the late Professor Soldano Ferrone, MD PhD, for his mentorship and advice. Although he is sorely missed, his significant impact on the field of immuno-oncology will always be remembered.

Conflict of Interest: None

Financial Support: The work was supported by Ministero dell' Università e della Ricerca, Progetti di Rilevante Interesse Nazionale (PRIN) 2017-COD. 2017PHRC8X_003 (to SP), PRIN 2020-COD. 2020ESS3F2_003 (to SP) and PRIN 2022-COD. 2022YWZWB2 (to SP).

Ethics Statement: The study was approved by "ASL Napoli 3 sud Servizio Coordinamento Etico Campania Sud" committee (prot./SCCE n.85275), in accordance with the Declaration of Helsinki and its amendments. All patients signed informed consent for clinical-pathological data acquisition. All patients signed informed consent for blood sample collection and analysis. Participants gave informed consent to participate in the study before taking part.

References

1. Bhatia A, Burtness B. Treating Head and Neck Cancer in the Age of Immunotherapy: A 2023 Update. Drugs (Abingdon Engl) 2023;83:217–48.
2. Borghaei H, Paz-Ares L, Horn L, et al. Nivolumab versus Docetaxel in Advanced Nonsquamous Non-Small-Cell Lung Cancer. N Engl J Med 2015;373:1627–39.
3. Brahmer J, Reckamp KL, Baas P, et al. Nivolumab versus Docetaxel in Advanced Squamous-Cell Non-Small-Cell Lung Cancer. N Engl J Med 2015;373:123–35.

4. Ferris RL, Blumenschein G Jr, Fayette J, et al. Nivolumab for Recurrent Squamous-Cell Carcinoma of the Head and Neck. N Engl J Med 2016;375:1856–67.
5. Lahiri A, Maji A, Potdar PD, et al. Lung cancer immunotherapy: progress, pitfalls, and promises. Mol Cancer 2023;22:40.
6. Motzer RJ, Escudier B, McDermott DF, et al. Nivolumab versus Everolimus in Advanced Renal-Cell Carcinoma. N Engl J Med 2015;373:1803–13.
7. Postow MA, Chesney J, Pavlick AC, et al. Nivolumab and ipilimumab versus ipilimumab in untreated melanoma. N Engl J Med 2015;372:2006–17.
8. Reck M, Rodríguez-Abreu D, Robinson AG, et al. Pembrolizumab versus Chemotherapy for PD-L1-Positive Non-Small-Cell Lung Cancer. N Engl J Med 2016;375:1823–33.
9. Robert C, Long GV, Brady B, et al. Nivolumab in previously untreated melanoma without BRAF mutation. N Engl J Med 2015;372:320–30.
10. Robert C, Schachter J, Long GV, et al. Pembrolizumab versus Ipilimumab in Advanced Melanoma. N Engl J Med 2015;372:2521–32.
11. Robert C, Thomas L, Bondarenko I, et al. Ipilimumab plus dacarbazine for previously untreated metastatic melanoma. N Engl J Med 2011;364:2517–26.
12. Novello S, Kowalski DM, Luft A, et al. Pembrolizumab Plus Chemotherapy in Squamous Non-Small-Cell Lung Cancer: 5- Year Update of the Phase III KEYNOTE-407 Study. J Clin Oncol 2023;41:1999–2006.
13. Garassino MC, Gadgeel S, Speranza G, et al. Pembrolizumab Plus Pemetrexed and Platinum in Nonsquamous Non-Small-Cell Lung Cancer: 5-Year Outcomes From the Phase 3 KEYNOTE-189 Study. J Clin Oncol 2023;41:1992–8.
14. Reck M, Ciuleanu T-E, Schenker M, et al. Five-year outcomes with first-line nivolumab plus ipilimumab with 2 cycles of chemotherapy versus 4 cycles of chemotherapy alone in patients with metastatic non-small cell lung cancer in the randomized CheckMate 9LA trial. Eur J Cancer 2024;211:114296.
15. Conroy M, Naidoo J. Immune-related adverse events and the balancing act of immunotherapy. Nat Commun 2022;13:392.
16. Williams KC, Gault A, Anderson AE, et al. Immune-related adverse events in checkpoint blockade: Observations from human tissue and therapeutic considerations. Front Immunol 2023;14:1122430.
17. Jia X-H, Geng L-Y, Jiang P-P, et al. The biomarkers related to immune related adverse events caused by immune checkpoint inhibitors. J Exp Clin Cancer Res 2020;39:284.
18. Valpione S, Pasquali S, Campana LG, et al. Sex and interleukin-6 are prognostic factors for autoimmune toxicity following treatment with anti-CTLA4 blockade. J Transl Med 2018;16:94.
19. Fujisawa Y, Yoshino K, Otsuka A, et al. Fluctuations in routine blood count might signal severe immune-related adverse events in melanoma patients treated with nivolumab. J Dermatol Sci 2017;88:225–31.
20. Diehl A, Yarchoan M, Hopkins A, et al. Relationships between lymphocyte counts and treatment-related toxicities and clinical responses in patients with solid tumors treated with PD-1 checkpoint inhibitors. Oncotarget 2017;8:114268–80.
21. Khan S, Khan SA, Luo X, et al. Immune dysregulation in cancer patients developing immune-related adverse events. Br J Cancer 2019;120:63–8.
22. Lim SY, Lee JH, Gide TN, et al. Circulating Cytokines Predict Immune-Related Toxicity in Melanoma Patients Receiving Anti-PD-1- Based Immunotherapy. Clin Cancer Res 2019;25:1557–63.
23. Pistillo MP, Fontana V, Morabito A, et al. Soluble CTLA-4 as a favorable predictive biomarker in metastatic melanoma patients treated with ipilimumab: an Italian melanoma intergroup study. Cancer Immunol Immunother 2019;68:97–107.
24. Bomze D, Hasan Ali O, Bate A, et al. Association Between Immune- Related Adverse Events During Anti-PD-1 Therapy and Tumor Mutational Burden. JAMA Oncol 2019;5:1633–5.
25. Gianchecchi E, Delfino DV, Fierabracci A. Recent insights into the role of the PD-1/PD-L1 pathway in immunological tolerance and autoimmunity. Autoimmun Rev 2013;12:1091–100.
26. Nielsen C, Laustrup H, Voss A, et al. A putative regulatory polymorphism in PD-1 is associated with nephropathy in a population-based cohort of

systemic lupus erythematosus patients. Lupus (Los Angel) 2004;13:510–6.

27. Kong EK-P, Prokunina-Olsson L, Wong WH-S, et al. A new haplotype of PDCD1 is associated with rheumatoid arthritis in Hong Kong Chinese. Arthritis Rheum 2005;52:1058–62.
28. Prokunina L, Castillejo-López C, Oberg F, et al. A regulatory polymorphism in PDCD1 is associated with susceptibility to systemic lupus erythematosus in humans. Nat Genet 2002;32:666–9.
29. Hashemi M, Karami S, Sarabandi S, et al. Association between PD-1 and PD-L1 Polymorphisms and the Risk of Cancer: A Meta-Analysis of Case-Control Studies. Cancers (Basel) 2019;11:1150.
30. Lee SY, Jung DK, Choi JE, et al. Functional polymorphisms in PD-L1 gene are associated with the prognosis of patients with early stage non-small cell lung cancer. Gene 2017;599:28–35.
31. Dong W, Gong M, Shi Z, et al. Programmed Cell Death-1 Polymorphisms Decrease the Cancer Risk: A Meta-Analysis Involving Twelve Case-Control Studies. PLoS One 2016;11:e0152448.
32. Zheng L, Li D, Wang F, et al. Association between hepatitis B viral burden in chronic infection and a functional single nucleotide polymorphism of the PDCD1 gene. J Clin Immunol 2010;30:855–60.
33. Common Terminology Criteria for Adverse Events (CTCAE). Protocol development. 2023. Available: https://ctep.cancer.gov/protocoldevelopment/electronic_applications/ctc.htm
34. Eisenhauer EA, Therasse P, Bogaerts J, et al. New response evaluation criteria in solid tumours: revised RECIST guideline (version 1.1). Eur J Cancer 2009;45:228–47.
35. Puca AA, Lopardo V, Montella F, et al. The Longevity-Associated Variant of BPIFB4 Reduces Senescence in Glioma Cells and in Patients' Lymphocytes Favoring Chemotherapy Efficacy. Cells 2022;11:294.
36. Nomizo T, Ozasa H, Tsuji T, et al. Clinical Impact of Single Nucleotide Polymorphism in PD-L1 on Response to Nivolumab for Advanced Non-Small-Cell Lung Cancer Patients. Sci Rep 2017;7:45124.
37. Pfaffl MW. A new mathematical model for relative quantification in real-time RT-PCR. Nucleic Acids Res 2001;29:e45.
38. Colangelo T, Carbone A, Mazzarelli F, et al. Loss of circadian gene Timeless induces EMT and tumor progression in colorectal cancer via Zeb1-dependent mechanism. Cell Death Differ 2022;29:1552–68.
39. Polcaro G, Liguori L, Manzo V, et al. rs822336 binding to C/EBPβ and NFIC modulates induction of PD-L1 expression and predicts anti-PD-1/PD-L1 therapy in advanced NSCLC. Mol Cancer 2024;23:63.
40. Hellmann MD, Rizvi NA, Goldman JW, et al. Nivolumab plus ipilimumab as first-line treatment for advanced non-small-cell lung cancer (CheckMate 012): results of an open-label, phase 1, multicohort study. Lancet Oncol 2017;18:31–41.
41. Sri-Ngern-Ngam K, Keawvilai P, Pisitkun T, et al. Upregulation of programmed cell death 1 by interferon gamma and its biological functions in human monocytes. Biochem Biophys Rep 2022;32:101369.
42. Bins S, Basak EA, El Bouazzaoui S, et al. Association between single-nucleotide polymorphisms and adverse events in nivolumab-treated non-small cell lung cancer patients. Br J Cancer 2018;118:1296–301.
43. Abdel-Wahab N, Diab A, Yu RK, et al. Genetic determinants of immune- related adverse events in patients with melanoma receiving immune checkpoint inhibitors. Cancer Immunol Immunother 2021;70:1939–49.
44. Refae S, Gal J, Ebran N, et al. Germinal Immunogenetics predict treatment outcome for PD-1/PD-L1 checkpoint inhibitors. Invest New Drugs 2020;38:160–71.
45. Boutros A, Carosio R, Campanella D, et al. The predictive and prognostic role of single nucleotide gene variants of PD-1 and PD-L1 in patients with advanced melanoma treated with PD-1 inhibitors. Immunooncol Technol 2023;20:100408.
46. Kobayashi M, Numakura K, Hatakeyama S, et al. Severe Immune- Related Adverse Events in Patients Treated with Nivolumab for Metastatic Renal Cell Carcinoma Are Associated with PDCD1 Polymorphism. Genes (Basel) 2022;13:1204.
47. Verzoni E, Cartenì G, Cortesi E, et al. Real-world efficacy and safety of nivolumab in previously-treated metastatic renal cell carcinoma, and association between immune-related adverse

events and survival: the Italian expanded access program. J Immunotherapy Cancer 2019;7:99.

48. Wu C-E, Yang C-K, Peng M-T, et al. The association between immune-related adverse events and survival outcomes in Asian patients with advanced melanoma receiving anti-PD-1 antibodies. BMC Cancer 2020;20:1018.
49. Horvat TZ, Adel NG, Dang T-O, et al. Immune-Related Adverse Events, Need for Systemic Immunosuppression, and Effects on Survival and Time to Treatment Failure in Patients With Melanoma Treated With Ipilimumab at Memorial Sloan Kettering Cancer Center. J Clin Oncol 2015;33:3193–8.
50. Riella LV, Paterson AM, Sharpe AH, et al. Role of the PD-1 pathway in the immune response. Am J Transplant 2012;12:2575–87.
51. Huang Y-F, Xie W-J, Fan H-Y, et al. Comparative Safety of PD-1/PD- L1 Inhibitors for Cancer Patients: Systematic Review and Network Meta-Analysis. Front Oncol 2019;9:972.
52. García Campelo MR, Arriola E, Campos Balea B, et al. PD-L1 Inhibitors as Monotherapy for the First-Line Treatment of Non-Small- Cell Lung Cancer in PD-L1 Positive Patients: A Safety Data Network Meta-Analysis. J Clin Med 2021;10:4583.